OPTIMIZATION OF PICOSECOND LASER PARAMETERS FOR SURFACE TREATMENT OF COMPOSITES USING A DESIGN OF EXPERIMENTS (DOE) APPROACH

Frank L. Palmieri[1], Rodolfo I. Ledesma[2], Joseph G. Dennie[3], Teersa J. Kramer[3], Yi Lin[4], John W. Hopkins[1], Christopher J. Wohl[1] and John W. Connell[1]

1. NASA Langley Research Center, Hampton, VA 23681
2. University of Virginia, Charlottesville, VA 22904
3. NASA Internship Program, Hampton, VA 23681
4. National Institute of Aerospace, Hampton, VA 23666

ABSTRACT

Based on guidelines from the Federal Aviation Administration, research supported by the NASA Advanced Composites Project is investigating methods to improve process control for surface preparation and pre-bond surface characterization on aerospace composite structures. The overall goal is to identify high fidelity, rapid, and reproducible surface treatments and surface characterization methods to reduce the uncertainty associated with the bonding process. The desired outcome is a more reliable bonded airframe structure, and to reduce time to achieve certification. In this work, a design of experiments (DoE) approach was conducted to determine optimum laser ablation conditions using a pulsed laser source with a nominal pulse width of 10 picoseconds. The laser power, frequency, scan speed, and number of passes (1 or 2) were varied within the laser system operating boundaries. Aerospace structural carbon fiber reinforced composites (Torayca® 3900-2/T800H) were laser treated, then characterized for contamination, and finally bonded for mechanical testing. Pre-bond characterization included water contact angle (WCA) using a handheld device, ablation depth measurement using scanning electron microscopy (SEM), and silicone contamination measurement using laser induced breakdown spectroscopy (LIBS). In order to accommodate the large number of specimens in the DoE, a rapid-screening, double cantilever beam (DCB) test specimen configuration was devised based on modifications to ASTM D5528. Specimens were tested to assess the failure modes observed under the various laser surface treatment parameters. The models obtained from this DoE indicated that results were most sensitive to variation in the average laser power. Excellent bond performance was observed with nearly 100% cohesive failure for a wide range of laser parameters. Below about 200 mW, adhesive failure was observed because contamination was left on the surface. For laser powers greater than about 600 mW, large amounts of fiber were exposed, and the failure mode was predominately fiber tear.

1. INTRODUCTION

Polymer matrix composites (PMC) have tremendous potential to improve the efficiency and performance of commercial transport airframes while reducing manufacturing cost and complexity through unitized construction and bonded assembly [1-2]. But the benefits of PMCs have not been fully realized due to concerns over the predictability of adhesive bond performance. In order to meet Federal Aviation Administration (FAA) certification criteria, secondary bonded, primary

structures (SBPS) are commonly drilled and mechanically fastened, at a significant cost [3-5]. Guidance from the FAA indicates improvements in process control and quality control would enhance bond predictability. FAA guidance to advance SBPS towards certification calls for improvements in process control and techniques for rapid analysis of bonding surface quality [6]. A repeatable, effective, and measurable surface treatment is a key component of an overall manufacturing methodology for the certification of SBPS [2, 5, 7].

1.1 Surface Preparation Techniques

1.1.1 General Remarks

Surface preparation for adhesive bonding removes contamination, imparts roughness, and chemically activates a surface to enhance adhesion. Methods such as solvent wiping, sanding, grit blast, and peel ply can remove contaminates, but often leave behind debris such as grit, polymer powder, or loose fibers that may be detrimental to bond performance [8-9]. Such methods also lack the reproducibility needed to for highly controlled, automated surface preparation [8].

1.1.2 Laser Ablation

Laser ablation is a method of using intense laser irradiation to remove contamination and surface layers similar to conventional grit blasting and sanding methods, but with no residual grit, no subsequent cleaning required, and with a high potential for automation [10-11]. Laser ablation is also highly selective such that contaminated matrix resin can be removed from a composite without damaging reinforcing fibers or causing significant exposure of fiber to the environment. Laser surface treatment is a readily automated, highly repeatable, and scalable solution to prepare composite surfaces for bonding [10-11]. Laser parameters such as power, focus, pulse frequency, and translation speed can be controlled and monitored in real time with a high degree of fidelity resulting in highly controlled and reproducible surface properties [10-13].

For ablation to occur, a laser pulse must have sufficient fluence (i.e. areal energy density) and power to reach the ablation threshold, above which an absorbing material is vaporized through several physical processes. The ablation threshold is a critical parameter for laser surface preparation and is highly material and laser process dependent. The laser fluence is affected by several process variables including: average laser power, pulse frequency, and spot size (focus). In addition to the fluence and power, other processing parameters such as surface coverage, and processing speed can impact surface preparation. Surface coverage and depth of removal are also dependent on spot size, scan speed, and pulse frequency. Because of the complex interdependencies of the ablation process on multiple variables, a DoE was used to model the dependence of laser process variables on surface properties and adhesive bond behavior.

Atmospheric pressure plasma (APP) surface treatment is another energetic means of preparing composite surfaces for bonding by oxidizing contaminates and matrix resin at the surface [8]. Unlike laser ablation, APP treatment converts silicones to oxidized and partially oxidized species, which are mostly non-volatile and remain on the surface. APP does not produce significant surface roughness and only interacts with the uppermost layers of a surface [14]. In contrast, the laser ablation process can be tuned to remove sub-micron to tens of microns of surface material with negligible or no thermal damage to the surface using picosecond or shorter pulse widths.

1.2 Silicone Contamination

Silicones (polydimethylsiloxane, PDMS) are ubiquitous in an industrial environment in seals, gaskets, release agents, lubricants, and even cosmetics used by employees. During demolding, silicone release agents are transferred to the surface of composite parts. In addition, volatile species can off-gas from silicone sources and condense on other surfaces. Silicones are highly detrimental to bond performance, and have been shown to deteriorate bond performance at contamination levels less than 10 $\mu g/cm^2$ [15] to less than 1 $\mu g/cm^2$ [11-12].

Silicone contamination was intrinsic to the surfaces of carbon fiber reinforced plastics (CFRP) substrates studied here, i.e. the contamination was accumulated using common composites fabrication techniques and through exposure to the laboratory environment. Previously reported X-ray photoelectron spectroscopy (XPS) data indicated an intrinsic silicone contamination of ~3.4 at% [16]. The silicone contamination was presumed to originate from release films and mold release agents regularly used in the composite fabrication processing facility.

1.3 Pre-bonding Surface Inspection

1.3.1 General Remarks

The means to rapidly determine if a treated composite surface is free of contaminants and chemically activated for bonding is a critical aspect improving bond predictability. The rapid detection of silicone contaminants on composites at the low concentrations mentioned in Section 1.2 is particularly challenging. Methods such as XPS and ion scattering spectroscopy can provide quantitative composition information for the uppermost atomic layers of a surface, but they are slow and require destructive sample preparation and stringent measurement conditions, making them impractical for manufacturing. Water contact angle (WCA) is being investigated as an in-line detection method of surface contaminant concentrations as low as 1 $\mu g/cm^2$ [15, 17]. The WCA measurement technique is non-destructive, rapid and sensitive to hydrophobic and hydrophilic contaminants. However, as mentioned previously, PDMS may diminish bond performance at concentrations less than 1 $\mu g/cm^2$. Therefore, WCA may not be quantitatively sufficient to detect ultralow level contaminants, especially considering additional interference from specimen surface topography, which strongly influences WCA and significantly reduces the certainty in the measurement.

1.3.2 Laser Induced Breakdown Spectroscopy

In addition to surface preparation, laser ablation also enables a characterization technique known as laser induced breakdown spectroscopy (LIBS) [11, 16]. LIBS measures the radiation emitted from the plasma plume formed during an ablation event in near real-time without any sample preparation or special atmospheric conditions. LIBS can measure residual silicone surface contamination at very low levels (< 1 $\mu g/cm^2$), and therefore, effectively detects silicone below the threshold concentration where bond performance may be compromised. The LIBS technique used here quantifies the silicone content on the surface in terms of the silicon-to-carbon (Si/C) ratio calculated from the silicon and carbon peak heights in the LIBS spectrum [11, 16]. LIBS is rapid and non-destructive, and could be integrated into a laser surface preparation system to provide real-time feedback of the surface composition or potentially be used for closed-loop control of the ablation process.

1.4 Contents of this Report

The process window for surface preparation of CFRP using a laser machining system with a picosecond pulse width was defined using a design of experiments (DoE) that identified 94 condition sets. The four factors used to define the surface treatment process were laser power, scan speed, pulse frequency, and number of passes. The responses that were measured were LIBS signal (Si/C), WCA, ablation depth and width, and failure mode after mechanical testing. To complete mechanical testing for all 94 test conditions efficiently, a rapid screening test method was developed to allow six conditions to be tested on each specimen with three replicates. Raw data and models from the DoE are presented and described.

2. EXPERIMENTATION

2.1 Materials

Double cantilever beam (DCB) specimens were fabricated from CFRP panels (30.5 cm × 30.5 cm, 12 in × 12 in) that were prepared from 10 plies of Torayca® P2302-19 prepreg tape (T800H/3900-2 carbon fiber/toughened epoxy resin system) and cured in an autoclave using the Toray® recommended cure cycle: 177 °C (350 °F) and 690 kPa (100 psi). Release from the caul plate was accomplished using Airtech A4000 release film [fluorinated ethylene propylene (FEP)]. The panels were laser treated and co-bonded within 48 h using Loctite® EA9696 film adhesive from Henkel Corporation and 10 additional plies of Torayca® P2302-19 prepreg tape. The co-bonded assemblies were cured in an autoclave following the Toray recommended cure cycle. The panels were subsequently cut into individual DCB specimens using a water jet.

2.2 DoE and Rapid Screening Methods

DoE software Design Expert® 10 was used to select ablation parameters and model the measured responses. Table 1 shows the variable ranges used to determine the 94 sets of laser parameters used in the DoE. To accelerate mechanical testing, the DCB test was adapted for rapid screening by: (1) including 6 process conditions on each test specimen and (2) using 3 replicates for each condition. This allowed for 12 process conditions to be tested on each 30 cm × 30 cm CFRP panel by laser processing a single 15.24 cm × 17.78 cm field as shown in Figure 1. Therefore, all 94 conditions could be tested with eight, co-bonded panels, resulting in 48 DCB specimens.

Table 1. The four laser process parameters and their associated ranges used in the DoE to determine the experimental test conditions.

Laser Parameter (units)	Range Tested
Average power (mW)	25 - 800
Pulse frequency (kHz)	200 - 1000
Scan speed (cm/s)	25.4 - 127
Number of passes	1 or 2

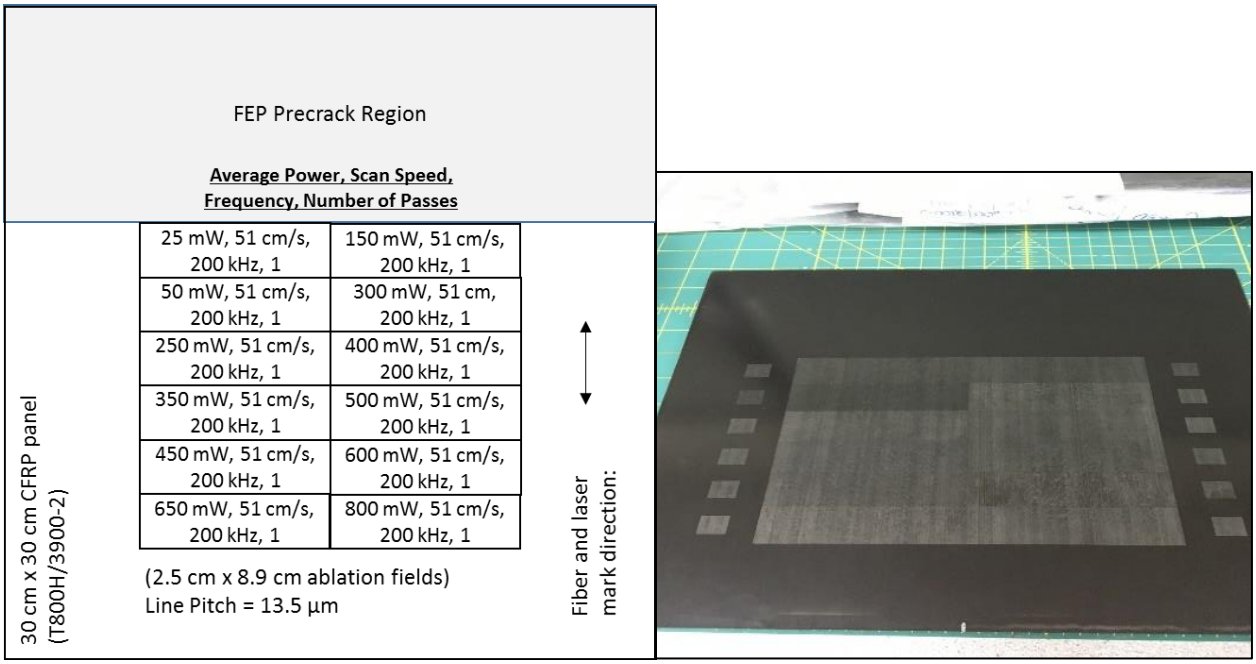

Figure 1. The diagram (left) shows the layout of the 12 ablation fields with the specified test conditions. Each field was 2.54 cm x 8.89 cm. The fiber/laser scan direction and the precrack region are indicated on the diagram. The photo (right) shows an example ablated panel with 12 ablated fields for mechanical testing and 12 additional fields (1.27 cm x 1.27 cm) for LIBS and WCA inspection.

2.3 Laser Processing

Laser treatment was performed on all panels using a PhotoMachining, Inc. system with a Ekspla, Atlantic 20, frequency tripled, Nd:YVO_4 laser source (6 W nominal average power at 355 nm and 200 kHz with ~10 ps pulse duration). A galvanometer was used to scan the laser spot across the stationary composite panels at a speed of 25.4 cm/s to 127 cm/s. The laser beam was focused by a 250 mm focal length f-theta lens (S4LFT6062/075, Sill Optics). A thermopile sensor (Model 3A) and Nova II power meter from Ophir-Spiricon LLC were used to monitor the average laser power. Laser ablation produced parallel lines in the fiber direction on unidirectional CFRP laminates. The line pitch was held constant for the DoE at 12.7 µm. The depth and width of laser of isolated lines ablated into CFRP was evaluated using a JEOL JSM 5600F SEM operated at an accelerating voltage of 10 to 15 kV (Figure 2). Specimens were coated with ~6 nm of Pd-Au for charge dissipation.

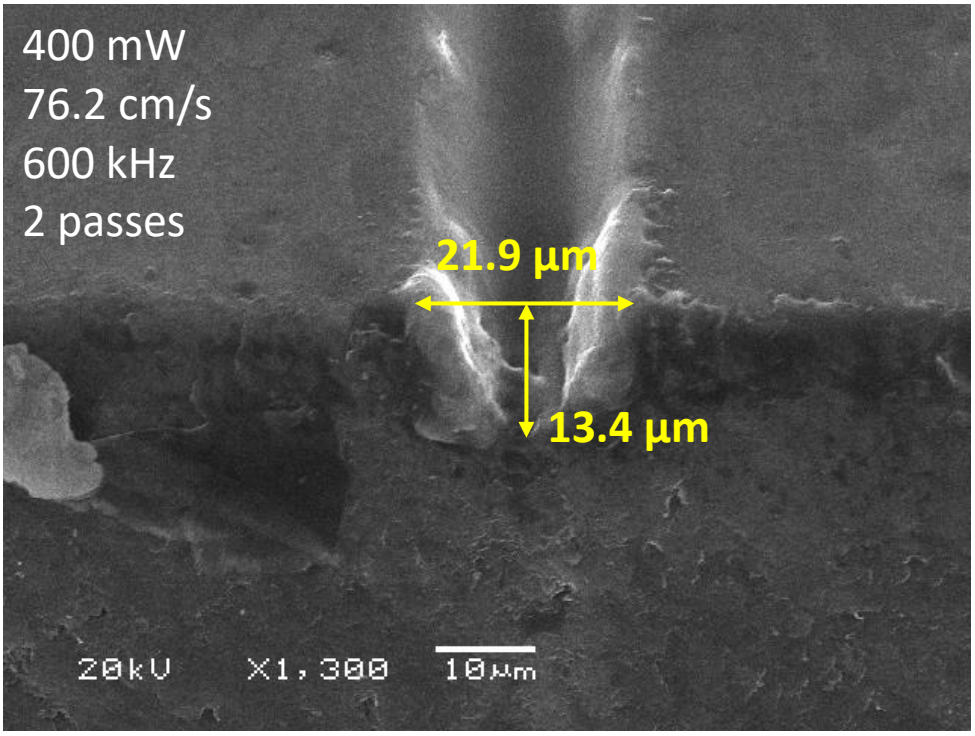

Figure 2. Scanning electron micrograph of an isolated line at a 45 degree view angle. Laser processing parameters are shown in the upper left-hand corner and measurements of the width and depth are indicated on the cross-section of the line. The measured depth was corrected for the error due to viewing at an angle.

2.4 Mechanical Testing

To create a crack starter, a 7.62 cm (3 in) long, 12.5 µm thick film of FEP was included in the layup during co-bonding of ablated panels. Using a modification of ASTM D5528-13, samples were machined with a water jet into six 2.5 cm x 24.1 cm (1 in x 9.5 in) specimens with notched ends for mounting directly onto a clevis grip, eliminating the need for bonding blocks, hinges or drilling [18]. To load the specimen onto the clevis grips, the specimen ends were opened ~4.4 mm prior to starting the test which resulted in a preload of 30 N to 40 N.

Prior to mechanical testing, one side of the test specimen was painted silver to enhance the visibility of the crack tip. The initial crack tip was marked by inspection with a 10× magnifying glass. An Instron® 5848 Microtester and 500 N load cell were used to record the applied load and displacement at a crosshead speed of 5 mm/min to an extension of 90 mm.

The failure modes of the rapid screening DCB specimens were analyzed to determine bond performance. Fracture toughness was not quantitatively assessed for the rapid screening test specimens because the maximum crack extension for each test condition (2.54 cm) was insufficient to develop steady state crack growth. Failed surfaces were scanned using an Epson V600 scanner at 24 bit color and 600 dpi resolution. The failure mode was digitally analyzed by grayscale threshold analysis using the ImageJ software, visual inspection, and guidance from ASTM D5573 [19]. An example of the failure modes observed on a rapid screening DCB sample is shown in Figure 3. To simplify the DoE models, similar failure modes were combined. Thin layer cohesive failure was combined with cohesive failure, and light fiber tear was combined with fiber tear

leaving only three distinct and complimentary failure modes to evaluate the full surface. Three replicates were averaged for each set of test conditions.

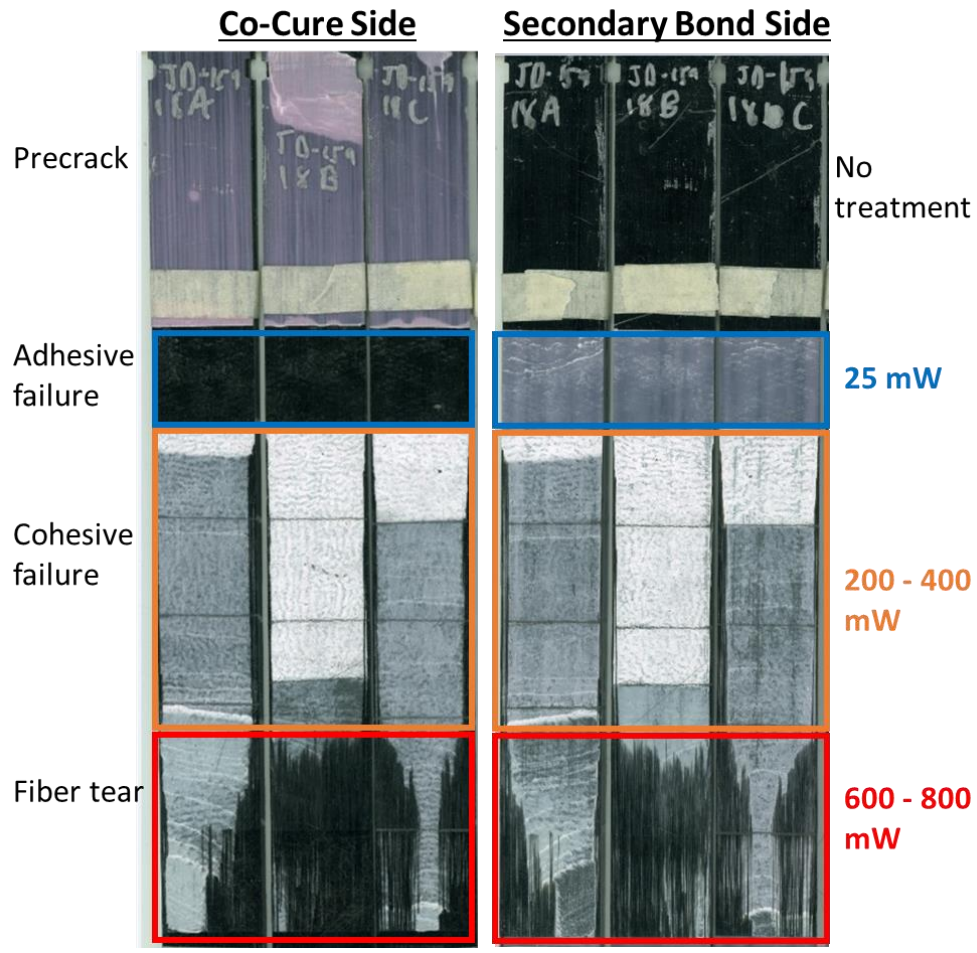

Figure 3. Example failure mode assessment of a failed rapid screening DCB sample (three specimens). Labels on the left of the figure indicate the dominant failure mode of the region in each colored rectangle. The labels on the right of the image indicate the average laser powers used to ablate the fields within each colored rectangle.

2.5 Contact Angle Measurement

WCAs were measured using a Surface Analyst™ device from BTG Labs. For all samples, WCAs were measured immediately following laser ablation on a 12.7 mm × 12.7 mm ablated field separated from the 15.24 cm × 17.78 cm ablation field used for mechanical testing. Nine WCA measurements were conducted for each test condition and the average value was incorporated into the DoE as the WCA response.

2.6 Laser Induced Breakdown Spectroscopy

The same laser system used for surface preparation was used as the excitation source for LIBS inspection. The radiant emission from the plasma plume formed during ablation was measured using a 328 mm, f/4.6 Schmidt-Czerny-Turner (SCT) spectrograph (IsoPlane SCT 320, Princeton

Instruments). The spectral response was recorded using an electron-multiplier intensified charge-coupled device (emICCD) camera (PI-MAX4: 1024 EMB, Princeton Instruments). The plasma emission was collected with a collimator and guided to the spectrograph via an optical cable with 19 fibers (200 μm each). A grating with 1200 grooves/mm, blazed at 300 nm, and a slit width of 10 μm was used to diffract the incident radiation collected from the plasma plume. The LIBS measurements were performed using a single laser shot with a pulse energy of 15 μJ (7.53 J/cm^2) at each inspection location. To improve the signal-to-noise ratio (SNR), 10 frames of 10 single laser shots were averaged by moving the sample under the stationary beam. The 10 single laser shots were accumulated on the CCD sensor. The aim of using a single shot on a fresh surface is to achieve high surface sensitivity [16].

3. RESULTS & DISCUSSION

3.1 DoE Model Results

Of the 94 test conditions specified in the DoE, 92 experiments were completed and contributed to the DoE model. A cubic model was used to fit the dependence of the six responses to the four laser parameters. All models were significant and had p-values less than 0.0001 as well as sufficient precision to navigate the design space.

Review of the modeled design space reveals some general relationships between the laser processing parameters and responses. The number of passes (1 or 2) was not found to correlate significantly with WCA or Si/C. Therefore, a laser process which removes contamination and promotes good bonds is not further improved by multiple passes. More importantly, a laser process that fails to remove contamination is not improved by repetition. The model also indicated that adhesive failure, Si/C, and WCA are relatively insensitive to changes in frequency or scan speed over the ranges tested. Assuming a minimum ablative spot size of 13 μm, the lowest frequency (200 kHz) and the highest scan speed (127 cm/s or 50 in/s) result in about 50% pulse overlap. The surface receives full coverage with the laser treatment even under the sparsest ablation condition. Above a critical power threshold, likely related to the ablation threshold, the surface treatment was effective independent of process speed.

All responses were found to depend strongly on laser power. The percentage of fiber tear failure mode increased nearly linearly with increasing average laser power and decreasing scan speed (Figure 4, right). The amount of fiber tear also correlated well with ablation depth. Above ~200 mW, no adhesive failure was observed (Figure 4, left) independent of scan speed. The percentage of adhesive failure decreased rapidly to zero as the average power increased above the ~200 mW threshold. A similar trend was observed for the Si/C response (Figure 5, right) which indicated nearly zero residual silicone contamination remained after ablation above an average laser power of ~200 mW. The similarity of the Si/C and adhesive failure responses indicated that the laser surface treatment had reduced the concentration of silicone contaminants below the detrimental threshold. The WCA results (Figure 5, left) showed curvature at both ends of the power spectrum. Like with Si/C and adhesive failure, the WCA also increased for laser powers less than 200 mW. In addition, the WCA decreased above 600 mW which may be attributed to an increase in exposed carbon fiber which increased with increasing laser power. Therefore, WCA appeared to be a useful

technique to characterize the removal of contamination and may also indicate the removal of the resin rich surface layer.

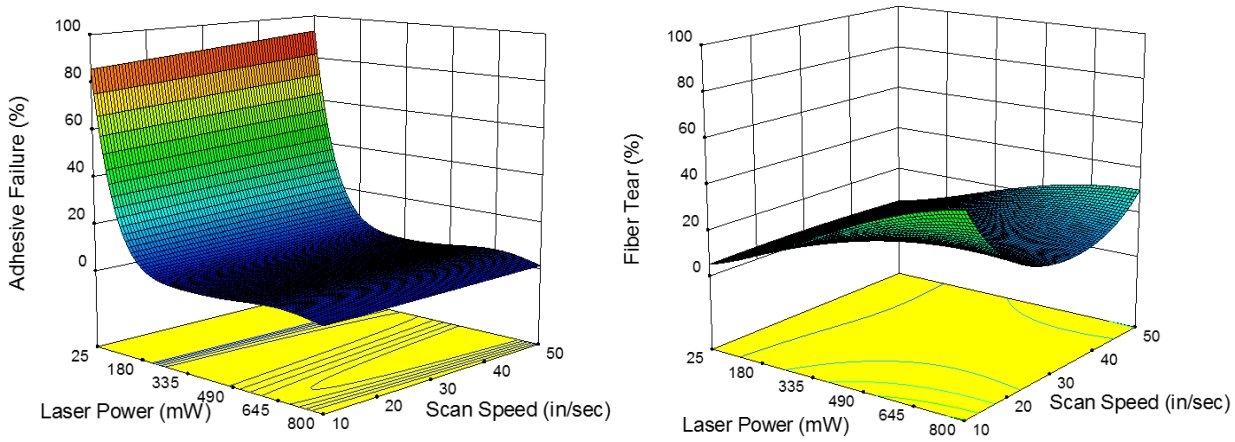

Figure 4. Surface plot from the DoE model showing the dependence of adhesive failure (left) and fiber tear (right) on scan speed and laser power for a frequency of 500 kHz and 1 pass. (1 in/s = 2.54 cm/s)

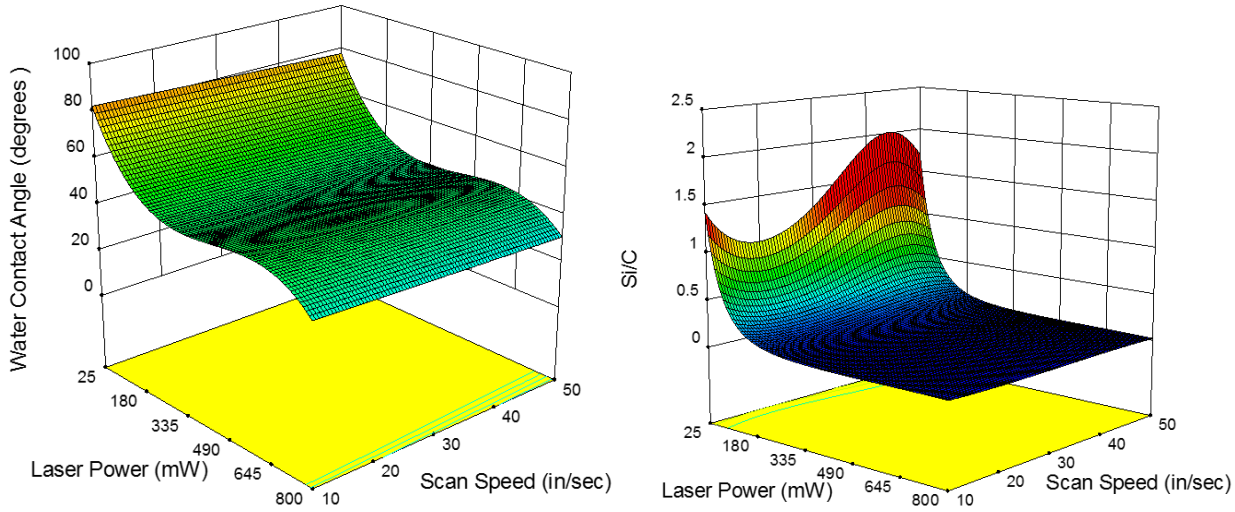

Figure 5. Surface plots from the DoE model showing the dependence of WCA (left) and Si/C (right) on scan speed and laser power for a frequency of 500 kHz and 1 pass. (1 in/s = 2.54 cm/s)

3.2 Optimization by DoE

The DoE models can also be used to select the most desirable laser parameters to optimize bond performance (i.e. minimize Si/C, adhesive failure, and fiber tear). For this optimization model, the greatest priority was placed on reducing adhesive failure and Si/C. Reducing fiber tear was a lower priority. The WCA, ablation width and ablation depth were not constrained for this optimization model. The desirability plot (Figure 6) shows that the process window was large, with highly desirable conditions occurring from about 250 mW to 800 mW with little dependence on scan speed. The most desirable parameters found for the optimization solution shown in Figure 6 are presented in Table 2.

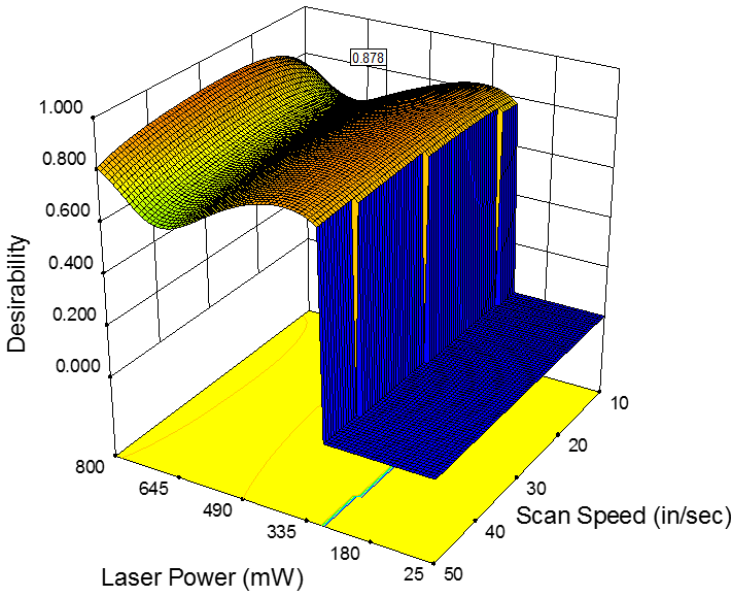

Figure 6. Surface plot of laser process desirability with scan speed and laser power for a frequency of 263 kHz and 1 pass. The label indicating the highest desirability on the plot reads 0.878. (1 in/sec = 2.54 cm/sec)

Although the highest desirability (0.88) occurred at 73 cm/s (28.7 in/s) scan speed, the flat dependence on scan speed suggests that the laser process could be operated at 127 cm/s (50 in/s) with minimal decrease in desirability. Based on this optimization, the maximum throughput of the laser system was limited by translation speed rather than power from the laser source. At the maximum scan speed of 127 cm/s (50 in/s) with a 12.7 µm line pitch, the throughput would be approximately 9.7 cm^2/min. At the maximum power of the laser source (6 W), the theoretical maximum throughput was 175 cm^2/min (~1 m^2/h). For comparison, an industrial picosecond laser source with a maximum power output of 100 W could theoretically achieve a processing rate of about 0.3 m^2/min.

Table 2. Optimized laser parameters and outputs.

Parameters	Value	Unit	**Output**	Value	Unit
Laser Power	374	mW	Adhesive Failure	2.0	%
Scan Speed	73	cm/s	Si/C	0.04	N/A
Frequency	263	kHz	WCA	44	Deg.
Number of Passes	1	N/A	Fiber Tear	7.4	%
			Ablation Depth	17.6	µm
			Ablation Width	17.6	µm

3.3 Comparison of Si/C and WCA Inspection

Although design models cannot be prepared to relate two response variables, interesting dependencies between response variables were observed. The dependencies of WCA and Si/C on adhesive failure are shown in Figure 7. WCA and Si/C were good predictors of adhesive failure, and poor bond performance was predicted by both techniques in all cases where it was observed

during mechanical testing. However, there was more scatter in the WCA data than the Si/C data. Contact angles ranged from ~10° to 70° (the maximum WCA in the DoE was 96°) for samples exhibiting negligible or no adhesive failure. The Si/C data ranged from 0 to 0.4 for samples exhibiting good bond performance (the maximum Si/C in the DoE was 1.44). The greater spread of the WCA data on surfaces that give good bonds could result in a high rate of false positives if this tool was used to detected contaminated surfaces. The surface roughness created by the laser treatment process may have affected the WCA measurement. The WCA and Si/C were both excellent tools to prevent the fabrication of weak bonds, but WCA alone was likely to result in a higher retreatment or scrap rate.

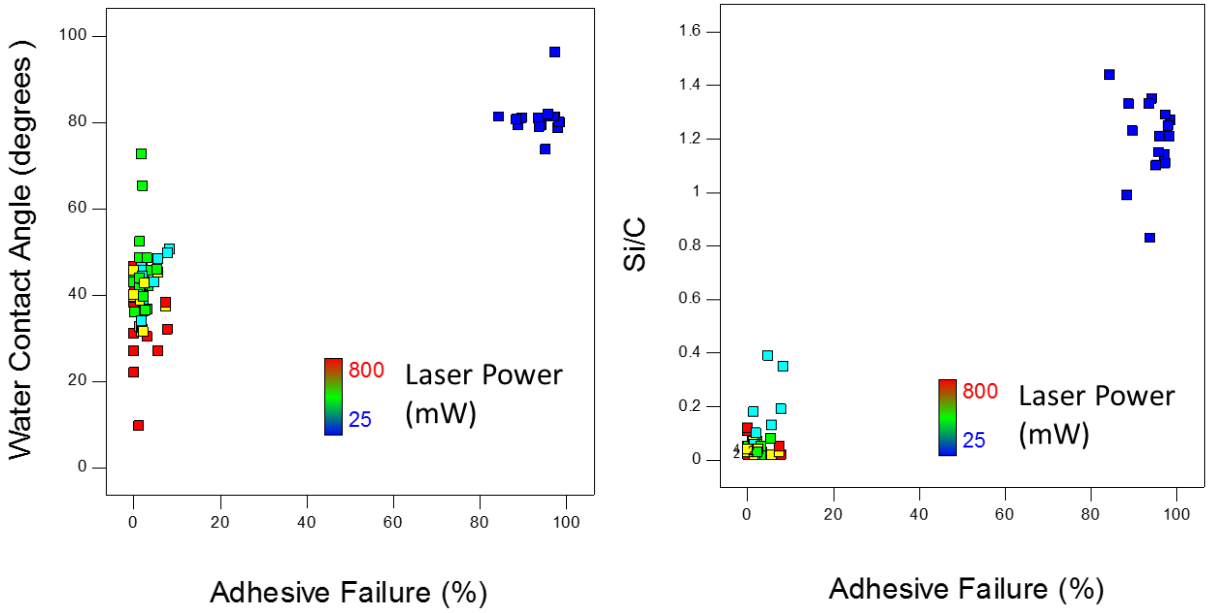

Figure 7. WCA and Si/C data with respect to adhesive failure mode observed in DCB specimens. The color of the points indicates the average laser power.

3.4 Ablation Depth and Width

The ablation width and depth were critical to the effectiveness of the laser surface treatment process. The width of an ablated line must be sufficient to allow adjacent lines to overlap each other such that no surface was left untreated. Even for a fully treated surface, the ablation depth was critical to the successful removal of contamination. Silicone, transparent to the 355 nm wavelength radiation produced by the laser, was not ablated during laser treatment. The underlying epoxy matrix, absorbing at 355 nm wavelength, carried away the silicone during ablation. Sufficient depth of the matrix resin must be removed from the surface to reduce the contamination level below the detrimental threshold. Excess ablation depth can expose reinforcing fibers to the environment. Although fiber exposure has not been shown to degrade bond performance, greater ablation depth does appear to correlate with increasing fiber tear failure mode in DCB testing (Figure 8).

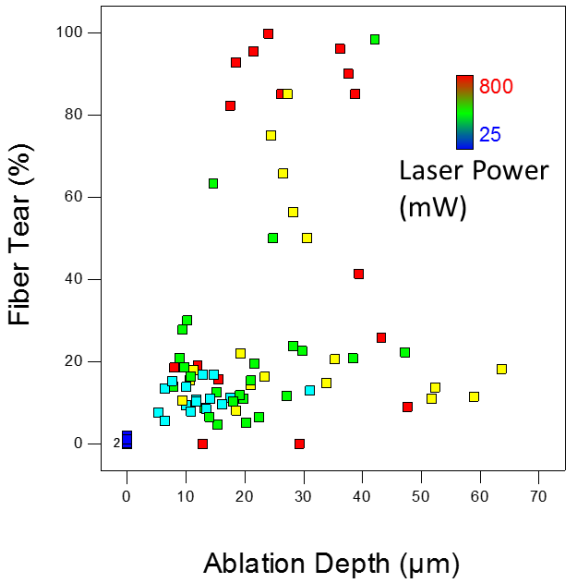

Figure 8. Fiber tear failure mode data with respect to ablation depth. The color of the points indicates the average laser power.

Models for the ablation depth and width are presented in Figure 9. The depth and width increased with increasing laser power up to about 400 to 500 mW. Ablation depth plateaued at about 30 µm, which was likely related to the average thickness of the resin rich layer on the surface of the CFPR panels. The maximum width ablated was about 20 µm, and depended primarily on the focus of the beam which was determined by optics of the laser system.

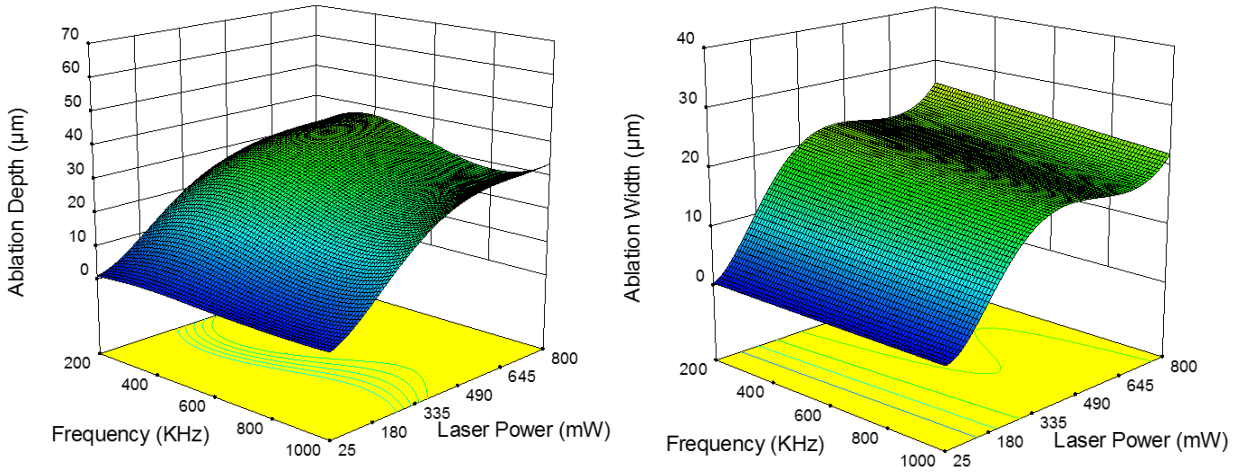

Figure 9. DoE models of the ablation depth (left) and the ablation width (right) measured from isolated lines using scanning electron microscopy are shown as a function of frequency and laser power. The number of passes was two and the scan speed was 76.2 cm/s (30 in/s).

4. CONCLUSIONS

Laser ablation is a robust technique for the removal of contamination from epoxy composite structures and promoting adhesive bonding/coating. The DoE indicated that average laser power

was the most critical parameter determining the removal of silicone contamination and bond performance. Nearly all process parameters tested above ~200 mW removed silicone and produced excellent bond performance regardless of scan speed, pulse frequency, and number of passes. Repetition of ablation processes (above or below the 200 mW threshold) did not significantly improve performance. Si/C ratio and WCA were both good predictors of adhesive failure. WCA data indicated less sensitivity and had more scatter compared to the Si/C data which was attributed to surface roughness. Surface preparation using the picosecond laser system was found to have a very broad process window to effectively remove silicone contamination from surfaces. Coupled with a facile LIBS inspection technique capable of quantifying ultralow level contaminants, laser ablation has excellent potential to improve the predictability of secondary bonded primary structure.

5. ACKNOWLEDGEMENTS

The work was supported by the NASA Advance Composites Project under the Advanced Aviation Program. The authors thank Sean Britton and Hoa Luong for sample fabrication, and Michael Oliver and Tom Hall for specimen preparation.

6. REFERENCES

1. Russell, J., "Advanced composite cargo aircraft proves large structure practicality." *Composites World* 12/04/2009, 2010.
2. Bossi, R. and Piehl, M. J., "Bonding primary aircraft structure: the issues." *Manufacturing Engineering* 2011, pp 101-109.
3. Gardiner, G., "Certification of bonded composite primary structures." *Composites World* 03/04/2014, 2014, p 8.
4. Gardiner, G., "Building TRUST in bonded primary structures." *Composites World* 04/01/2015, 2015, p 5.
5. Kruse, T., Fuertes, T. A. S., Koerwien, T. and Geistbeck, M. "Bonding of CFRP primary aerospace structures - boundary conditions for certification in relation with new design and technology developments," *Proceedings of the 2015 International SAMPE Tech. Conf.* Seattle, WA, 2014 Society for the Advancement of Materials and Process Engineering. CD-ROM. 15 pp.
6. Advisory Circular Number 20-107B, 2010 Federal Aviation Administration. Washington, DC, 2010.
7. Piehl, M. J., Bossi, R. H., Blohowiak, K. Y., Dilligan, M. A. and Grace, W. B. "Efficient certification of bonded primary structure," *Proceedings of the 2013 International SAMPE Tech. Conf.* Long Beach, CA, 2013 Society for the Advancement of Materials and Process Engineering. CD-ROM. 649-658 pp.
8. Belcher, M. A. T., Krieg, K. L., Voast, P. J. V. and Blohowiak, K. Y. "Nonchemical surface treatments using atmostpheric plasma systems for structural adhesive bonding," *Proceedings of the 2013 International SAMPE Tech. Conf.* Long Beach, CA, 2013 Society for the Advancement of Material and Process Engineering. CD-ROM. 5 pp.
9. Higgins, A., "Adhesive bonding of aircraft structures." *International Journal of Adhesion & Adhesives* **2000,** *20*, 367-376.
10. Palmieri, F., Ledesma, R., Cataldo, D., Lin, Y., Wohl, C., Gupta, M. and Connell, J. "Controlled contmaination of epoxy composites with PDMS and removal by laser ablation,"

Proceedings of the 2016 International SAMPE Tech. Conf. Long Beach, CA, 2016 The Society for the Advancement of Materials and Process Engineering. CD-ROM. 14 pp.
11. Palmieri, F., Ledesma, R., Fulton, T., Arthur, A., Eldridge, K., Thibeault, S., Lin, Y., Wohl, C. J. and Connell, J. W. "Picosecond pulsed laser ablation for the surface preparation of epoxy composites," *Proceedings of the 2017 International SAMPE Tech. Conf.* Seattle, WA, 2017 Society for the Advancement of Materials and Process Engineering. CD-ROM. 14 pp.
12. Palmieri, F. L., Belcher, M. A., Wohl, C. J., Blohowiak, K. Y. and Connell, J. W., "Laser ablation surface preparation for adhesive bonding of carbon fiber reinforced epoxy composites." *International Journal of Adhesion and Adhesives* **2016,** *68*, 7.
13. Palmieri, F. L., Watson, K. A., Morales, G., Wohl, C. J., Williams, T., Hicks, R. and Connell, J. W., "Laser ablative surface treatment for enhanced bonding of Ti-6Al-4V alloy." *ACS Applied Materials and Interfaces* **2012,** *5* (4), 1254-1261.
14. Williams, T. S., Yu, H., Yeh, P. C., Yang, J. M. and Hicks, R. F., "Atmospheric pressure plasma effects on the adhesive bonding properties of stainless steel and epoxy composites." *Journal of Composite Materials* **2014,** *48* (2), 219-233.
15. Oakley, B., Bichon, B., Clarkson, S., Dillingham, G., Hanson, B., McFarland, J. M., Palmer, M. J., Popelar, C. and Weatherston, M. "Determination of threshold levels of archetype contaminant compounds on composite adhereds and their quantification via FTIR and contact angle techniques," San Antonio, TX, 2016 Annual Meeting of the Adhesion Society. 3 pp.
16. Ledesma, R. I., Palmieri, F. L., Connell, J. W., Yost, W. T. and Fitz-Gerald, J., "Surface characterization of carbon fiber reinforced polymers by picosecond laser induced breakdown spectroscopy." *Spectrochim. Acta, Part B* **2017,** *140*, 7.
17. Oakley, B., Bichon, B., Clarkson, S., Dillingham, G., Hanson, B., McFarland, J. M., Palmer, M. J., Popelar, C. and Weatherston, M. "TRUST - A novel approach to determine effects of archetype contaminant compounds on adhesion of structural composites," *Proceeding of the 2015 International SAMPE Tech. Conf.* Baltimore, MD, 2015 Society for the Advancement of Material and Process Engineering. 12 pp.
18. ASTM Standard D5528-13, 2013, "Standard test method for mode I interlaminar fracture toughness of unidirectional fiber-reinforced matrix composites" ASTM International, West Conshohocken, PA, 2013, www.astm.org.
19. ASTM Standard D5573-99, D5573-ADJ 1999, "Standard Practice for Classifying Failure Modes in Fiber-Reinforced-Plastic (FRP) Joints" ASTM International, West Conshohocken, PA, 1999, www.astm.org.